Wear Behavior Analysis of Imperfect Functionally Graded Parts: Analytical and Experimental Techniques

Emad Kadum Njim[1*], *Muhsen* J. Jweeg[2] , *Mohammed* H. Al-Maamori[3] , *Zainab* S. Idan[4], *Muhannad* Al-Waily[5], *Ahmed* Mouthanna[6] and *L.* Hadji[7]

[1]Ministry of Industry and Minerals, State Company for Rubber and Tires Industries, Iraq
[2]Al-Farahidi University, College of Technical Engineering, Iraq
[3]Biomaterials Engineering Department, Engineering College, University of Al-Mustaqbal, Iraq
[4]Department of Computer Technical Engineering, college of Technical Engineering, university of Akafeel, Al-Najaf, Iraq,
[5]Department of Mechanical Engineering, Faculty of Engineering, University of Kufa, Iraq
[6]College of Engineering, University of Anbar, Ramadi, Anbar, IRAQ.
[7]Department of Mechanical Engineering, University of Tiaret, Tiaret, Algeria

Abstract. A combination of an analytical solution and experimental tests was used in this study to evaluate the wear resistance of a porous functionally graded material (PFGM) structural system.A cylindrical porous sample is fabricated using 3D printing technology based on different parameters. According to ASTM standards, the sliding wear behavior of porous samples has been investigated using a Pin on the Disc Tribometer. The results showed reasonable agreement between experimental and analytical analyses, with a discrepancy of 10.434 %. This indicates that 3D printing can be suitable for manufacturing reliable viscoelastic samples. However, the porosity parameter has a significant influence on wear resistance. The porous gradation technique led to a higher experimental wear resistance of around 31% for FGM PLA samples.Morphological observation on specimen fracture surfaces was done using a scanning electron microscope (SEM) to check the PFGM layer's nature.

1 Introduction

Controlling friction and wear in moving machine parts is a critical industry issue. Surface wear occurs when two solid surfaces slide, roll, or impact against one another, resulting in material loss or damage. Wear occurs most often due to the interaction between surfaces with irregularities. Several mechanisms in cutting tool wear have not yet been fully identified or understood [1].

Metal, polymer, and functionally graded materials (FGM) sandwich structures are recommended as excellent designs for bending and dynamic loads [2]. In almost every engineering application, FGMs are ideal due to their essential characteristics. The thermal and mechanical properties of FGMs make them suitable for a wide range of applications, and they may find new ones in the future. The existing applications include aerospace, automobiles, energy, defense, electrical/electronics, marine, biomedical, and automotive [3].

A manufacturing process can result in pores and micro-voids inside FGM plates, reducing their strength considerably. As far as cost-benefit ratios are concerned, sintering is the most commonly used method of producing FGM. A structure made of PFGM can reduce its weight and improve its mechanical properties due to its graded porosity. Porosity gradient functionally graded materials (PFGMs) are types of viscoelastic materials in which the porosity of the material changes in a specified direction. They are widely used in biomedical, aerospace, automobile, and energy applications [4]. Porous materials have two phases: a solid phase containing atoms or molecules and a void phase containing air, gas, or another substance, such as water. In traditional measurements, porosity percentage is used to determine the physical properties of porous materials [5, 6].

The wear tests have a wide range of applications. A wear machine of the Okoshi type measures the wear resistance of FGMs reinforced with hybrid Al3Ti/Al3Ni platelets. An investigation of hybrid Al–(Al3Ti+Al3Ni) FGMs was described in this study [7]. According to Tayyebi and Alizadeh (2023), accumulative and cold-roll bonding can be combined to make a new method based on cold-roll bonding [8]. Güler et al. (2021) studied their arc-erosion performance using hot-pressing to fabricate functionally graded copper-based electrical contact materials. A cylindrical

* Corresponding author: emad-njim@scrit.gov.iq

disk with a concentric hole and a functionally graded material disk are investigated here for their thermoelastic behavior [9].

Other authors studied the wear behavior of functionally graded Al alloy/Al2O3 and the impact of fabricating method parameters on the overall performance [10]. According to Ferreira et al., 2011, functionally graded materials (FGMs) made by centrifugal machining exhibit microstructure and tribocorrosion behavior. Results indicate that higher mechanical wear leads to higher corrosion relative amounts [11]. ANOVA and Taguchi optimization methods are successfully used to analyze the wear characteristics of FGMs. The wear data is also validated using artificial neural networks (ANNs). Tests are conducted with pin-on-disc machines under a variety of conditions, including sliding velocity (1.57–3.66 m/s), average applied force (10–30 N), reinforcement material (0–20 wt.%), and sliding distances (1–3 km) [12].

The experiments were designed to analyze the impact of variables on the specific wear rate of Al6061 + SiC and Al6061 + V2O5 based on the Taguchi Design of Experiments (DOE) and artificial neural network approach [13]. Under diverse loads and speeds and different concentrations of materials, the wear behavior of polyester composites containing glass fibers was studied using adaptive neuro-fuzzy inference systems [14]. ANNs have also been used to model and predict composites' Tribological properties, providing researchers with insight into what they can expect in the future [15]. The wear resistance of composite FGM structures has attracted many researchers recently. Radhika et al. (2023) Conducted a study using horizontal centrifugal casting to examine the performance of homogeneous and FG composites. The wear behavior was assessed on a linear reciprocating tribometer without lubrication while adjusting process parameters and considering average load and sliding distance [16]. The hardness and wear properties of Al-12Si-Cu/B4C FGMs were analyzed by Radhika and Raghu, 2016, concluding that the hardness gradually increased from the outer to the inner periphery [17].

Abdulmajeed and Hamzah (2022) investigated the Tribological properties of functionally graded nanocomposite samples containing different volume fractions of Al2O3. This study compared graded composites with homogeneous filling and graded composites with graded filling based on their hardness and wear parameters. Comparatively, the wear rate of functionally graded specimens showed a noteworthy improvement of 87.7% compared to neat epoxy loaded from the side rich in alumina, as indicated by the tests conducted. The literature concludes that limited research has been conducted on the reciprocating wear behavior of FG composites, with restricted experiments specifically focusing on reciprocating wear. Furthermore, experimental tests and comparative evaluations were conducted on the FGM's three distinct regions (outer, middle, and inner) and the homogeneous castings. The impact of the weight fraction of reinforcements on the material properties of various materials (metallographic, mechanical, and Tribological) was examined and presented [18].

M.H. Nie et al. investigated the wear mechanism and microstructure of 316/NiTi FGM samples [19]. The FGM with gradient layers demonstrates better wear resistance at both low- and high speeds than 316 substrates due to the superelasticity and high hardness of intermetallic compounds, resulting in slighter oxidative and abrasive wear. Recently, many researchers have successfully prepared gradient structures to study the wear performance of inhomogeneous alloys [20,21].

P. Pradhan et al. [22] examined the behavior of an indenter coated with functionally graded material (FGM) and a rigid half-space under plane-strain conditions. They used a series solution approach to analyze the 2D contact using a singular integral equation. Unlike the commonly used piecewise constant material properties, they proposed a piecewise linear FGM modeling method with a modified Fourier series, which proves to be a more precise and effective way to represent FGM material properties. In their study, G.H. Majzoobi et al. [23] analyzed the Tribological properties of functionally graded material (FGM) samples. Specifically, they examined Titanium/Hydroxyapatite (Ti-HA) and Ti-SiO2 FGM samples fabricated using three die compaction techniques for potential use in dental implants. Microscopic observations revealed that adhesion, delamination, and abrasion were the primary wear mechanisms observed in all FGM samples. The researchers concluded that the Ti-HA sample produced through the Split Hopkinson Bar method exhibited superior tribological properties comparable to natural human teeth. In their study, P.F. Jiang et al. [24] focused on the successful preparation of a corrosion-wear-resistant alloy steel gradient material for a camshaft using the direct laser deposition technique. They employed various analytical tools to analyze these properties, such as X-ray diffraction, electron backscatter diffraction, a hardness tester, and a wear tester. The results showed that an increase in the gradient parameter promoted the toughness and enhanced the wear resistance of the tested sample.

Furthermore, numerous studies in previous literature have examined the wear of functionally graded materials (FGM) [25,26]. The mechanical and tribological behavior of five-layered two-phase Aluminium and Copper FGM produced by powder metallurgy was studied by Vasavi Boggarapu et al. [27]. The results indicated that Al/Cu FGM samples exhibited superior friction and wear characteristics over base materials. Using an artificial neural network, Ismail Najjar et al. predicted the tribological properties of (Al-TiO2) nanocomposite samples tested at four different wear loads [28].

Composites with various particle sizes are tested for dry sliding wear at speeds of 80 mm/s, 110 mm/s, and 140 mm/s and four normal loads of 5 N, 10 N, 20 N, and 30 N, respectively [29]. By changing the wear mechanism from abrasion to delamination, increased loads and sliding speeds increased wear severity. According to the analysis of variance (ANOVA), the load was the most significant parameter of the volume loss. Similarly, the tribological properties of Al matrix hybrid nanocomposites with multiple reinforcement particles were investigated [30]. It is found that the wear resistance of composites is improved in the Al matrix with the presence of graphene particles.

The motivation of the current research is to prepare single-phase porous functionally graded materials with varying porosity content and power-law indices. Multiple process parameters were tested in the study while considering the

effects of average load and sliding distance, allowing for the evaluation of wear behavior on an unlubricated linear reciprocating Tribometer. Numerical results are presented for a Steel/, Al, and Polymer FGM disk, and the effects of the priority distribution profile, volume fraction index, angular speed of the disk, and geometrical properties of the disk are analyzed in detail. In order to characterize wear debris and worn surfaces, scanning electron microscopy (SEM) was used to examine their morphology. Various polymer composites' mechanical and physical properties were thoroughly examined, and the wear resistance based on multiple parameters was evaluated. Among the outcomes, the study revealed valuable insights into the wear resistance exhibited by porous functionally graded parts.

2 Analytical Formulation

To understand the context, consider a functionally graded material (FGM) disc made of one constituent, such as rubber or thermoplastic polymer (Polylactic acid (PLA)), commonly found in biological tissues. Many techniques are essential during the analysis to examine the wear behavior of the PFGM structure. According to equation 1, the recommended rule for the volume fraction according to the porosity distribution (Ω) might be considered to be in the form of a cylindrical with a diameter (d), changing through z direction and by adopting a power-law distribution scheme (n).

$$V_p(z) = V_m - \Omega . V_m \left(\frac{z}{r} + \frac{1}{2}\right)^n \quad (1)$$

Vp is the entire volume fraction of porous metal, Vm is the volume fraction of base metal, and n denotes a power-law variation explaining the change in the thickness of material properties. In the current investigation, the novel PFGM disk comprises only one component (single phase) [31, 32].
Polymer metal with an equal distribution of the porosity volume fraction (Ω) should be graded through the radial direction only. Hence, for example, n = 0, Vp (z) = Vm while n =∞, (Vp=Vm=1). Consequently, the proposed mechanical properties of the PFGM beam can be represented as follows:

$$\emptyset(z) = \emptyset_m - \Omega . \emptyset_m \left(\frac{z}{r} + \frac{1}{2}\right)^n \quad (2)$$

Øm denotes the metal material property of the Porous functionally graded disk. Thus, for the homogeneous beam (Ω= 0), whereas for the imperfect VE disk, the material characteristics of the PFGM circular part, Young's modulus (E), and mass density (ρ) may be represented as

$$E(z) = E_m - E_m \Omega \left(\frac{z}{r} + \frac{1}{2}\right)^n \quad (3)$$

$$\rho(z) = \rho_m - \rho_m . \Omega \left(\frac{z}{r} + \frac{1}{2}\right)^n \quad (4)$$

3 Materials and Methods

3.1 Materials

FGM and homogeneous polymers were processed using PLA, TPU, PEEK30% CF, and ABS. Using a 3D printer machine type (Creality CR-10 V3). The printing parameters are displayed in Table 1, while Table 2 shows the fabricated components' elemental properties. These thermoplastic polymers offer a good combination of mechanical and thermal properties at high and low temperatures due to their excellent hardness, resistance, wear and mechanical erosion, and thermal stability. The Archimedes principle was applied to measure functional density for various homogenous polymers. The density of the epoxy and the FGPNC samples were experimentally determined by implementing Archimedes' principle. Each PFGM sample was weighed in the air. After this, samples were placed in a crucible filled with distilled water for two minutes to remove air bubbles. After that, distilled water was used to determine the weight. A weight loss in water was attained when the discrepancy between the measurements was determined by Archimedes' principle [33].

3.2 Experimental Testing and Analysis

According to the feature of density variation through sample layers, porous functionally grade composite samples with various FG parameters and geometrical properties were fabricated through a 3D printing machine. In this work, polylactic acid (PLA) polymer filament with a diameter of 1.75 mm manufactured by China was the raw material for creating hardness and wear tests using an Ender - 3D printer machine. The 3D printed specimens were designed, exported as STL files, and imported into a 3D printing machine using SolidWorks software. Figures (1a and 1b) show the processing procedure of FGM wear samples, while the printing settings used for each sample are displayed in Table 1.

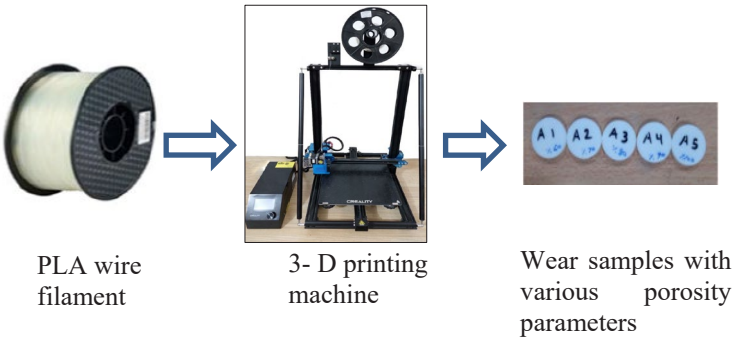

Fig. 1a. Flow chart of fabrication polymer wear samples.

The instrument used is a Pin-on-disk Tribometer with a maximum vertical force of 200 N, 750 watts, and Rotational speed from 0 to 2000 rpm. Figure 2 illustrates the experimental wear setup. From this test, the wear resistance and coefficient of friction can be obtained based on various parameters such as normal applied load, rotational speed, and distance. The test standards for each set of samples were applied to three samples in total. Averaging over three measurements has been used to prepare the results presented here. The composites were also fabricated according to the standard (ASTM D2240) for the hardness (Shore D) test.

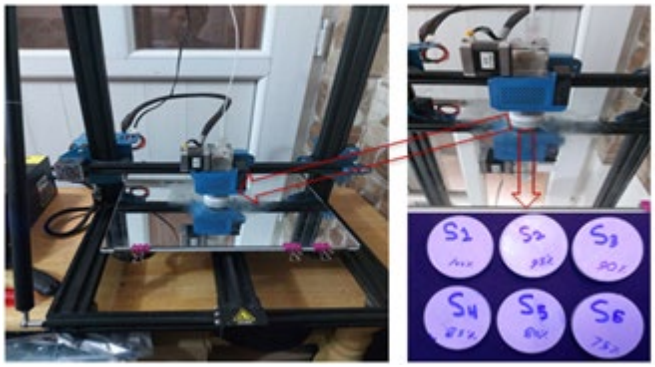

Fig. 1b. Fabrication of wear samples using a 3-D printing machine (ASTM G 99) [34].

Pin-on-disc friction experiments were conducted using an unlubricated reciprocating wear test bench (Model MT/60/NI/HT/L). Experiments were carried out for all PFGM and homogenous castings according to various parameters, including applied load (10, 20, and 30 N) and rotation speed (200, 300, 400, and 500 rpm). The sliding distance was determined as a function of the (30 - 120) minute test duration. Through experimental procedure and sample preparation, ASTM G99 standards were used with the polished surfaces of the samples. In a pin-on-flat Tribometer, a cylindrical pin with a 10 mm diameter was used as a specimen against flat steel of the EN 31 type.
A hard carbide pin with a diameter of 10 mm and a hardness of 2.5 GPa serves as the counter surface. A strain gauge is used to measure the friction force during the test by measuring the deflection of the elastic arm; hence, the friction coefficient can be determined and recorded with the help of suitable software. Before testing, the surfaces of both the sample and the pin were washed with acetone and thoroughly dried. The sample set was initially weighed with an electronic balance to an accuracy of ± 0.0001 gm. A (+0.1, -0.1) mg-accurate precision electronic balance was used to measure material loss from the composite surface.
All tests were carried out at room temperature and without lubrication. The friction coefficient (μ) is calculated through the experiment by measuring the friction force employing the deflection of the elastic arm with the help of a strain gauge.
Slip wear loss is measured by the beginning and ultimate weight difference. Each set of utilized test standards was applied to three samples. The findings presented are the average of three measurements.
The formula (Wear rate = wear volume / Normal load per sliding distance) was used to calculate the wear rate (Ws) [35].

$$W_s = \frac{v}{F \times x} = \frac{m^3}{N.m} \qquad (5)$$

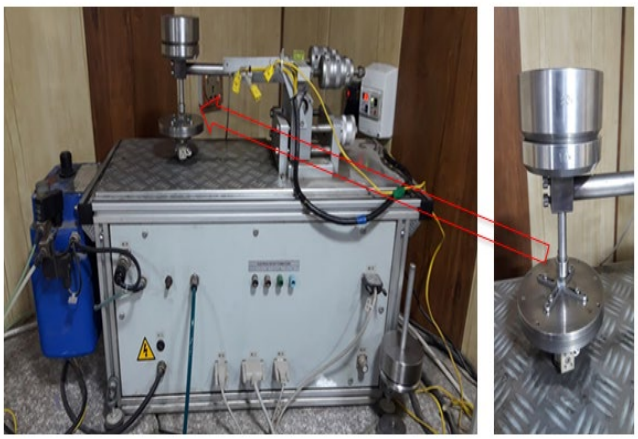

Fig. 2. The wear test setup using the wear test bench (Model MT/60/NI/HT/L) Sliding Machine.

4 Results and Discussions

This research presents comparable experimental and theoretical analysis data for evaluating the effect of porous functionally graded parameters on Tribological characteristics.
The following examples explain the testing results of wear characteristics of the porous functionally graded cylindrical specimen using the analytical solution in conjunction with experimental results.

Example 1: Under a normal load of 20 N and 500 revolutions per minute for 50 hours, the flat face of a 30 mm-diameter FGM porous Aluminium (n=1, Ω =0.1) disc is rotated about its axis. (The hardness of the steel is 2.5 GPa, the density of the steel is 7.8 Mg/m3, the hardness of the aluminum is 0.8 GPa, and the density of the aluminum is 2.7 Mg/m3). The aluminum and steel mass losses were 15 mg and 2 mg during the test. Calculate the steel and aluminum wear depths and coefficients of friction [36].

Solution

The anticipated scenario during the test load involves the load being supported by plastic contacts in a PFG Al-steel contact. In this regard, the wear coefficients can be calculated as follows:

W = 10 N
Aluminum mass loss (ma)=15 milligrams,
Steel mass loss (ms) = 2 milligrams,
500 rpm is the rotational speed,
Test duration: 50 hours,

$$v_a = \frac{m}{\rho}\, m^3$$

$$v_a = \frac{15 \times 10^{-3}}{2.7 \times 10^3}\, m^3 = 5.56 \times 10^{-6}\, m^3$$

$$v_s = \frac{2 \times 10^{-3}}{7.8 \times 10^3}\, m^3 = 2.56 \times 10^{-7}\, m^3$$

The contact diameter= 30 mm and the average sliding distance, x = π × 30 × 10−3 × 500 × 50 × 60m = 14.13 *104 m.
The wear coefficient for both materials can be calculated as follows:

$$k_a = \frac{\mathrm{v_a} \times \mathrm{H_a}}{\mathrm{W.x}} = \frac{5.56 \times 10^{-6} \times 0.8 \times 10^9}{20 \times 14.13 \times 10^4} = 1.57 \times 10^{-3}$$

$$k_s = \frac{\mathrm{v_s} \times \mathrm{H_s}}{\mathrm{W.x}} = \frac{2.56 \times 10^{-7} \times 2.5 \times 10^9}{20 \times 14.13 \times 10^4} = 2.27 \times 10^{-4}$$

$$d_a = \frac{\mathrm{v_a}}{\mathrm{A_a}} = \frac{5.56 \times 10^{-6}}{\pi(15)^2 \times 10^{-6}}\mathrm{m} = 7.86\ \mathrm{mm}$$

$$d_s = \frac{v_s}{A_s} = \frac{2.56 \times 10^{-7}}{\pi(15)^2 \times 10^{-6}} \text{m} = 0.363 \text{ mm}$$

$$W_s = \frac{5.56 \times 10^{-6}\, m^3}{20 \times (14.13 \times 10^4)} = 1.967 \times 10^{-3} \text{ mm}^3/\text{N.m.}$$

Example 2: Find the amount of porous FG Polytetrafluoroethylene (PTFE) volume displaced for each unit slid distance when a rigid steel surface, consisting of conical asperities with an average semi-angle of 60°, glides on a softer PTFE surface under a load of 10 N. Furthermore, calculate the wear coefficient of PTFE using the given data that 10−6 m3 of PTFE material is extracted during a sliding distance of 1 Km, n =1, Ω =0.1.

Solution

Given the roughness angle, θ = 30° , n=1, Ω =0.1 , Load W = 10N , v PTFE = 10−6 m3 , H PTFE = 49 Kg/mm2, at the n=1, Ω =0.1 , H PTFE1 = 47 Kg/mm2.

The volume of material displaced by all asperities in unit slid distance is

$$v = \frac{2W.\overline{\tan\theta}}{\pi.H_{PTFE1}} = \frac{2 \times 10 \times \tan 30}{\pi \times 460.9125 \times 10^6} \text{ m}^3/\text{m}$$

$$= 8.1256 \times 10^{-9} \text{ m}^3/\text{m}$$

The wear coefficient of porous FG (PTFE) polymer is

$$k_{abr} = \frac{v_{PTFE} \times H_{PTFE}}{W.x}$$

$$k_{abr} = \frac{10^{-6} \times 460.9125 \times 10^6}{10 \times 10^3}$$

$$= 0.461$$

$$W_s = \frac{10^{-6}\, m^3}{10 * 10^3} = 10^{-1} \text{ mm}^3/\text{N.m}$$

Figure 3 shows the friction coefficient experimental results of the perfect FG (PLA) samples, which vary with the power law index under normal load (10 N) at a fixed radius-to-depth ratio (r/h = 5). This figure clarifies that the volume fraction exponent impacts the coefficient of friction of perfect samples. The same behaviour can be obtained with even porosity distribution samples.

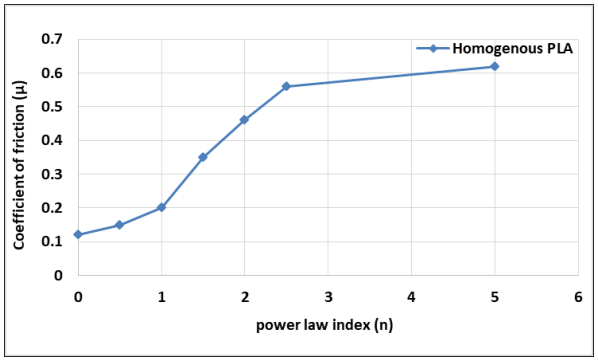

Fig. 3. Variation of coefficient of friction of PLA samples with the indenter having a zero porosity and various power-law index.

Example 3: In order to explicitly understand the porosity effect on the wear behavior of PFG cylindrical samples with the exact dimensions mentioned in example 1, made of various polymers (PLA, TPU, PEEK 30% CF, ABS), samples are tested first for hardness, then subjected to normal load 10 N and 400 revolutions per minute for 2 hours. The disc is rotated about its axis. Calculate the steel and each polymer wear depths and coefficients of friction according to the following information:
Power law index (n=1), the porosity parameter (Ω =0.1), Each polymer and steel mass loss during the test were 25 mg and 1 mg, respectively. Table 2 shows the mechanical properties of tested polymers.

Solution:

By using Eq. 2, the hardness of each polymer type can be found at n=1, Ω =0.1, following the same procedure in example 1. The results are recorded in Table 3. From the results, it can be seen that the ABS polymer type has a higher

wear rate. The possible reason is stiffness and less density than other types. For this reason, it is widely used in automobile manufacturing.

The wear resistance obtained using the current solution is in excellent agreement with the experimental results, as shown by an analysis of Table 4. It has been noted that a rise in the gradient index's value results in a fall and a decrease in the wear coefficient. Additionally, it has been stated that solid cylinders cause the wear factor to increase. The result shows that 0.3 % PLA-filled porous-based FGMs exhibit the lowest specific wear rate among all the fabricated FG composites. However, it can be seen that an increase in the power-law index from 0 to 5 leads to a decrease in the specific wear by (8.5, 17.42, and 26.53 %) at porosity parameters (0.1, 0.2, and 0.3), respectively. The maximum discrepancy between theoretical and experimental solutions is 10. 434 % occurred at n =0.5, Ω=0.2.

In polymers, the influence of porosity on wear resistance depends on the specific application and material properties. In some cases, increasing porosity can improve wear resistance. Porous polymers can act as sacrificial layers that absorb wear and protect the underlying material.

Additionally, the porosity can distribute loads and reduce contact pressure, minimizing wear. However, excessive porosity can lead to reduced mechanical properties, reduced strength, and increased susceptibility to crack initiation and propagation, resulting in poor wear resistance. Reducing porosity through proper processing techniques is necessary in such cases to enhance wear resistance.

Table 5 shows the results of the specific wear rate of four porous polymers (PLA, TPU, PEEK 30 % CF, and ABS) using three values of porosity parameters (Ω=0.1, 0.2, and 0.3) and various FG exponents (n =0, 0.5, 1, 2, and 5). The results show that the wear rate decreased by increasing the power law index and improved by the porosity parameter; the possible reason is the increased rigidity of the polymer by increasing the power law index and reducing the voids inside the desired polymer samples.

Furthermore, from the results, one can conclude that several factors determine the specific behavior of composite material, including its reinforcing phase, the characteristics of the FG layers, and the processing conditions used during manufacturing. Hence, optimizing the volume fraction index requires carefully considering these factors to achieve the desired wear resistance in metals and polymers.

Minimizing or controlling porosity generally improves wear resistance in metals and polymers. This can be achieved through appropriate material selection, processing techniques, and quality control measures to ensure denser and more homogeneous materials.

Table 1. Printing parameters are used for all mold sample manufacturing.

Nozzle dia. (mm)	Layer thickness (mm)	Infilling density	Infilling pattern	Printing temp. (C°)	Bed Temp. (C°)	Printing speed mm/sec
0.40	0.28	100%	lines	200	60	50

Table 2. Mechanical properties of different polymers used.

Polymer type	Hardness (shore D) kg/mm2	Density (kg/m3)
PLA	85	1240
TPU	68	1210
PEEK 30%CF	88	1410
ABS	77	1030

Table 3. Analytical results of the wear coefficients of various porous polymer types placed on a flat carbon steel plate for power-law exponent (n =1) and porosity parameter (Ω=0.1).

Polymer type	v1(m3)	v2(m3)	k1	k2	d1 (m)	d2 (m)	Ws (mm3/N.m)
PLA	2.122e-5	1.282e-7	3.728e-7	7.088e-3	0.0300	1.815e-4	4.694e-1
TPU	2.175e-5	1.282e-7	3.066e-7	7.088e-3	0.0310	1.815e-4	4.810e-1
PEEK 30%CF	1.866e-5	1.282e-7	3.400e-7	7.088e-3	0.0264	1.815e-4	4.128e-1
ABS	2.555e-5	1.282e-7	4.045e-7	7.088e-3	0.0362	1.815e-4	5.651e-1

Table 4. Analytical and experimental results of the wear coefficients of porous (PLA) placed on a flat carbon steel plate for various power-law exponents (n) and porosity parameters (Ω).

Porosity factor	Power law index (n)									
	0		0.5		1		2		5	
	Ana.	Exp.	Ana.	Exp.	Ana.	Exp.	Ana.	Exp.	Ana.	Exp.
0	0.446	0.466	0.446	-	0.446	-	0.446	-	0.446	-

0.1	0.495	0.535	0.478	0.525	0.469	0.496	0.461	0.497	0.453	0.487
0.2	0.557	0.588	0.515	0.575	0.495	0.538	0.477	0.512	0.46	0.505
0.3	0.637	0.675	0.559	0.598	0.525	0.559	0.495	0.545	0.468	0.498

Table 5. Analytical results of the wear coefficients of porous FG polymers placed on a flat carbon steel plate for various power-law exponents (n), porosity parameters (Ω), and FG porous metal.

Mat.	**Porosity factor**	**Power law index (n)**				
		0	**0.5**	**1**	**2**	**5**
PLA	0	0.446	0.446	0.446	0.446	0.446
	0.1	0.495	0.478	0.469	0.461	0.453
	0.2	0.557	0.515	0.495	0.477	0.460
	0.3	0.637	0.559	0.525	0.495	0.468
TPU	0	0.457	0.457	0.457	0.457	0.457
	0.1	0.508	0.490	0.481	0.472	0.464
	0.2	0.571	0.528	0.508	0.489	0.472
	0.3	0.653	0.573	0.538	0.507	0.480
PEEK 30%CF	0	0.392	0.392	0.392	0.392	0.392
	0.1	0.436	0.420	0.413	0.405	0.398
	0.2	0.490	0.453	0.436	0.420	0.405
	0.3	0.560	0.491	0.461	0.435	0.411
ABS	0	0.537	0.537	0.537	0.537	0.537
	0.1	0.597	0.576	0.565	0.555	0.545
	0.2	0.671	0.621	0.596	0.575	0.554
	0.3	0.767	0.673	0.632	0.595	0.563

Figures (4 to 7) show that a scanning electron microscope (SEM) was used to characterize the surface microstructure of PFGM samples with various porosity distributions; for example, at (Ω=0.2), and gradient index (n =1), the PLA samples damaged due to sliding wear test was examined. To examine the topography of wear-damaged sample surfaces, the secondary electron test (SE) method provides a useful tool, and a backscattered electron test (BSE) was conducted in the current study. As a result of atomic number differentiation, BSE can carry information on the sample's magnetic field. The results suggest cracks propagate in both planes and transverse directions due to sliding wear occurring at the PLA samples.
It is important to note that pores' size, distribution, and interconnectedness also affect wear resistance. Large or interconnected pores are more detrimental to wear resistance than small, isolated ones. Additionally, the type of wear (e.g., abrasive, adhesive, erosive) and the wear mechanisms involved can also impact the relationship between porosity and wear resistance.

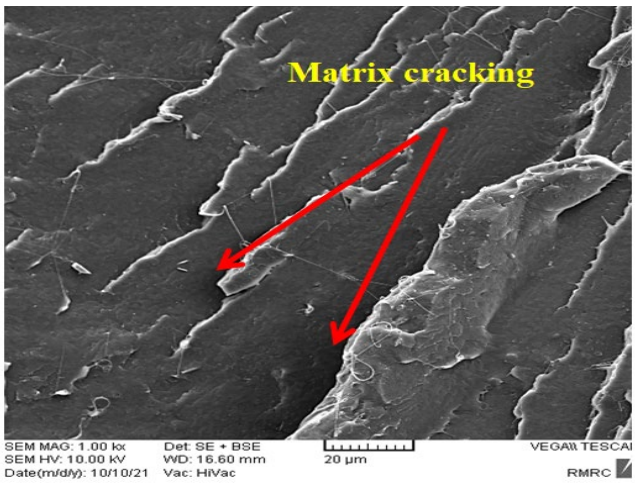

Fig. 4. The surface microstructures of the PLA sample, at 34.8 mm WD and 1mm depth at porosity 0.2

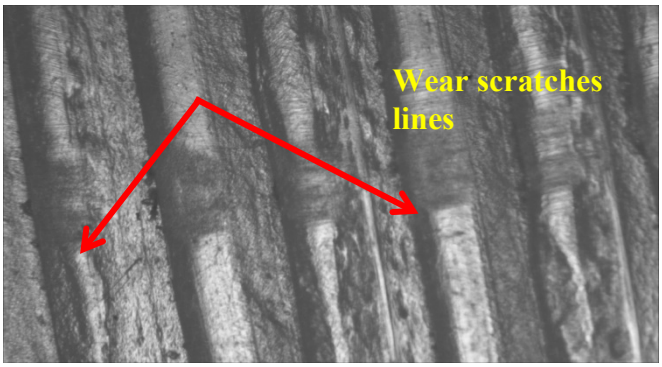

Fig. 5. The surface microstructures of the PLA sample at porosity 0.2.

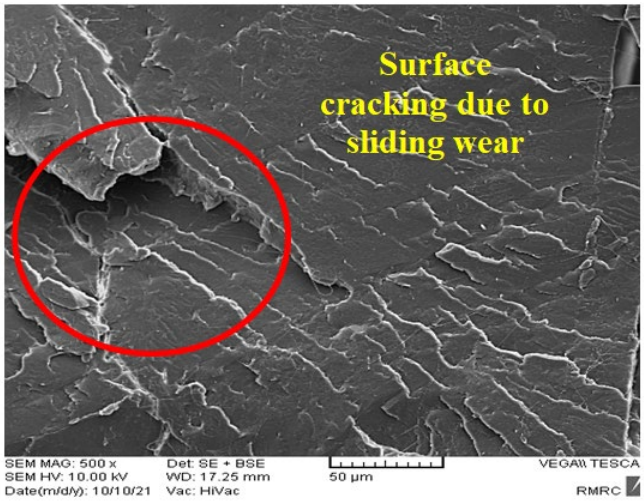

Fig. 6. The surface microstructures of the PLA sample, at 16.6 mm WD, 20µm depth at porosity 0.2.

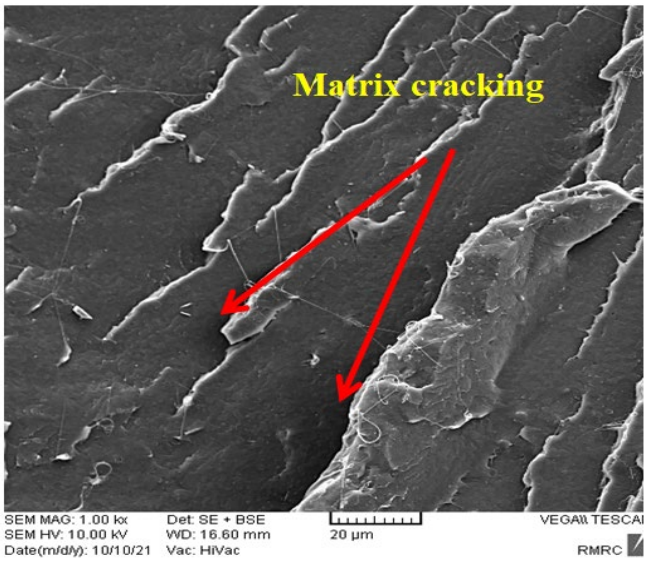

Fig. 7. The surface microstructures of the PLA sample, at 15.69 mm WD, 10µm depth at porosity 0.2.

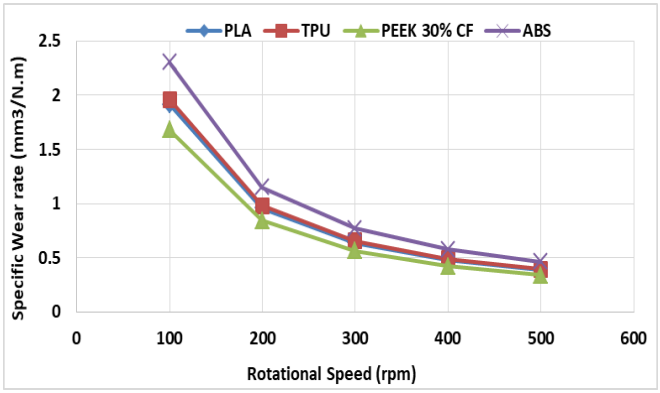

Fig. 8. Variation of specific wear various porous polymers at (n =0.5, Ω=0.1)

Using the same data employed in example 2 but at the power-law index (n=0.5), the relation between rotational speed and wear resistance for various polymer types at porosity 10 % is given in Fig. 8. The results showed that the highest wear appeared at the ABS polymer type, possibly due to its fewer influences by void content and indicating the significance of hardness properties. The impact of wear test time is illustrated in Fig. 9. Samples with a porosity of 15 %, gradient index of 10, load of 10 N, and rotational speed of 250 rpm are analyzed to determine the wear resistance at various durations. The same behavior can be noticed where the ABS sample exhibits the highest wear resistance compared to other porous polymer types due to the metallurgical nature of the internal microstructure.

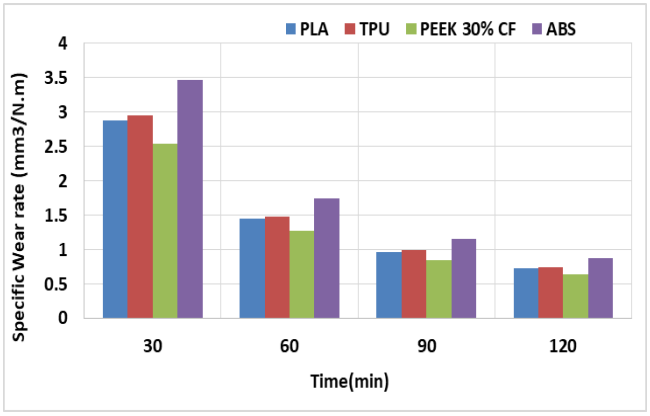

Fig. 9. Influence of time variation on the specific wear of various porous polymers at (n=10, Ω=0.15), 250 rpm, 10 N.

5 Conclusions

The Wear, like friction, is a system reaction rather than a material property. Interface wear is affected by operating conditions. It is frequently assumed incorrectly that high-friction interfaces have high rates of wear. This isn't always the case. For instance, ceramics exhibit moderate friction but shallow wear, unlike interfaces with solid lubricants and polymers, which display relatively low friction and high wear.

In our case, we have four parameters: normal load, speed, FG parameters, and test time. It has been discovered that the FG parameter and porous polymer type can play a sustained wear resistance. We emphasize that achieving these results depended on the excellent selection of these parameters. Wear rate is typically used to quantify the wear process. The amount of material removed per unit of time or sliding distance is known as the wear rate. Other forms, like material depth per unit sliding distance or volume removed per apparent contact area and unit sliding distance, may not have a dimension. In general, the wear rate is not constant. The rate of wear is typically a complicated function of time.

There are several ways to improve the wear resistance of porousFG polymers:

- Enhancing wear resistance by adding filler materials: Adding fibers such as glass, carbon, or nanoparticles can make polymers significantly more wear-resistant. The polymer matrix is strengthened and more resistant to wear with these fillers.
- An improvement in wear resistance can be achieved by modifying the polymer's surface. Plasma treatment or thin film coatings can increase the hardness and durability of polymer surfaces.
- Polymers and other surfaces can be lubricated to reduce friction and wear. Incorporate solid lubricants and oils into the polymer matrix or incorporate self-lubricating materials.

Additional research is required to clarify the influence of all material and test parameters, as well as those related to the microstructure of the tested materials, on the use of the multi-pass dual-indenter method in the variant proposed in this paper. A strategy will be tried through energetic models of plastic deformation during the abrasion of the two steels.

Acknowledgement

The authors thank the Ministry of Industry, a state company of Iraq's rubber and tire industries, and the University of Babylon, Faculty of Materials Engineering, Iraq, for experimental work and technical and equipment support.

References

1. S. Mezlini, P. Kapsa, J.C. Abry, C. Henon, C., and J. Guillemenet, “Effect of indenter geometry and relationship between abrasive wear and hardness in early stage of repetitive sliding,” Wear, vol. 260, no. (4-5), pp. 412-421, 2006.
2. M. J. Jweeg, E. K. Njim, O. S. Abdullah, M. A. Al-Shammari, M. Al-Waily, and S. H. Bakhy, “Free Vibration Analysis of Composite Cylindrical Shell Reinforced with Silicon Nano-Particles: Analytical and FEM Approach,” Physics and Chemistry of Solid State, vol. 24, no. 1. Vasyl Stefanyk Precarpathian National University, pp. 26–33, Feb. 23, 2023.
3. E. K. Njim, S. H. Bakhy H. S., M. Al-Waily, “Experimental and numerical flexural analysis of porous functionally graded beams reinforced by (Al/Al2O3) nanoparticles,” International Journal of Nanoelectronics and Materials, vol. 15, no. 2, pp. 91-106, 2022.
4. E. Kadum Njim, S. Emad, and M. N. Hamzah, “A Recent Review Of The Sandwich-Structured Composite Metamaterials: Static And Dynamic Analysis,” Jurnal Teknologi, vol. 85, no. 5. Penerbit UTM Press, pp. 133–149, Aug. 21, 2023.
5. E. K. Njim, “Analytical and numerical flexural properties of polymeric porous functionally graded (PFGM) sandwich beams,” Journal of Achievements in Materials and Manufacturing Engineering, vol. 110, no. 1. Index Copernicus, pp. 5–10, Jan. 01, 2022.
6. H. Raad, E. K. Njim, M. J. Jweeg, and M. Al-Waily, “Sandwiched Plate Vibration Analysis with Open and Closed Lattice Cell Core,” Physics and Chemistry of Solid State, vol. 24, no. 2. Vasyl Stefanyk Precarpathian National University, pp. 312–322, Jun. 19, 2023.
7. Y. Watanabe and T. Nakamura, “Microstructures and wear resistances of hybrid Al–(Al3Ti+Al3Ni) FGMs fabricated by a centrifugal method,” Intermetallics, vol. 9, no. 1. Elsevier BV, pp. 33–43, Jan. 2001.
8. M. Tayyebi and M. Alizadeh, “Thermal and wear properties of Al/Cu functionally graded metal matrix composite produced by severe plastic deformation method,” Journal of Manufacturing Processes, vol. 85. Elsevier BV, pp. 515–526, Jan. 2023.
9. O. Güler, T. Varol, Ü. Alver, and S. Biyik, “The wear and arc erosion behavior of novel copper based functionally graded electrical contact materials fabricated by hot pressing assisted electroless plating,” Advanced Powder Technology, vol. 32, no. 8. Elsevier BV, pp. 2873–2890, Aug. 2021.
10. B. Kumar, A. Joshi, K. K. S. Mer, L. Prasad, M. K. Pathak, and K. K. Saxena, “The impact of centrifugal casting processing parameters on the wear behavior of Al alloy/Al2O3 functionally graded materials,” Materials Today: Proceedings, vol. 62. Elsevier BV, pp. 2780–2786, 2022.
11. S. C. Ferreira, P. D. Sequeira, Y. Watanabe, E. Ariza, and L. A. Rocha, “Microstructural characterization and tribocorrosion behavior of Al/Al3Ti and Al/Al3Zr FGMs,” Wear, vol. 270, no. 11–12. Elsevier BV, pp. 806–814, May 2011
12. A. K. Singh, Siddhartha, and S. Hussain, “Wear Peculiarity of TiO2 Filled Polyester-Based Homogeneous Composites and their Functionally Graded Materials Using Taguchi Methodology and ANN,” Materials Today: Proceedings, vol. 2, no. 4–5. Elsevier BV, pp. 2718–2727, 2015.
13. R. U. Baig, S. Javed, A. Kazi, and M. Quyam, “Artificial neural network approach for the prediction of wear for Al6061 with reinforcements,” Materials Research Express, vol. 7, no. 7. IOP Publishing, p. 076503, Jul. 01, 2020.
14. S. Yilmaz, R. Ilhan, and E. Feyzullahoğlu, “Estimation of adhesive wear behavior of the glass fiber reinforced polyester composite materials using ANFIS model,” Journal of Elastomers & Plastics, vol. 54, no. 1. SAGE Publications, pp. 86–110, Jun. 09, 2021.
15. U. M. R. Paturi, S. Cheruku, and N. S. Reddy, “The Role of Artificial Neural Networks in Prediction of Mechanical and Tribological Properties of Composites—A Comprehensive Review,” Archives of Computational Methods in Engineering, vol. 29, no. 5. Springer Science and Business Media LLC, pp. 3109–3149, Jan. 29, 2022.
16. N. Radhika and R. Raghu, “Development of functionally graded aluminum composites using centrifugal casting and influence of reinforcements on mechanical and wear properties,” Transactions of Nonferrous Metals Society of China, vol. 26, no. 4. Elsevier BV, pp. 905–916, Apr. 2016.

17. N. Radhika, J. Sasikumar, J. Sylesh, and R. Kishore, "Dry reciprocating wear and frictional behavior of B4C reinforced functionally graded and homogenous aluminum matrix composites," Journal of Materials Research and Technology, vol. 9, no. 2. Elsevier BV, pp. 1578–1592, Mar. 2020.
18. A. M. Abdulmajeed and A. F. Hamzah, "Hardness and Dry Sliding Wear Characterization of Functionally Graded Materials Employing Centrifugal," Materials Science Forum, vol. 1077. Trans Tech Publications, Ltd., pp. 57–67, Dec. 15, 2022.
19. M. H. Nie, P. F. Jiang, Y. X. Zhou, Y. L. Li, and Z. H. Zhang, "Studies on the 316/NiTi functionally gradient ultra-thick coatings fabricated with directed energy deposition: Microstructure, crystallography and wear mechanism," Applied Surface Science, vol. 630. Elsevier BV, p. 157497, Sep. 2023. doi: 10.1016/j.apsusc.2023.157497.
20. M. H. Nie et al., "Achieving illustrious friction on a directed energy deposition 316/NiTi heterogeneous alloy with bionic Ni interlayer," Applied Surface Science, vol. 638. Elsevier BV, p. 158107, Nov. 2023. doi: 10.1016/j.apsusc.2023.158107.
21. Z. Chen, Z. Sun, J. Yang, J. Zhang, and X. Yao, "Research on the microstructure and properties of iron based alloy coatings based on gradient transition," Vibroengineering Procedia, vol. 50. JVE International Ltd., pp. 194–199, Sep. 21, 2023. doi: 10.21595/vp.2023.23436.
22. P. Pradhan, A. IR, and H. Murthy, "Modeling of FGM contacts using piecewise linear variation in Young's modulus," Tribology International, vol. 186. Elsevier BV, p. 108645, Aug. 2023. https://doi.org/10.1016/j.triboint.2023.108645
23. G. H. Majzoobi, K. Rahmani, M. Mohammadi, H. Bakhtiari, and R. Das, "Tribological behavior of Ti/HA and Ti/SiO2 functionally graded materials fabricated at different strain rates," Biotribology, vol. 35–36. Elsevier BV, p. 100233, Dec. 2023. https://doi.org/10.1016/j.biotri.2022.100233
24. P. F. Jiang, C. H. Zhang, S. Zhang, J. B. Zhang, J. Chen, and Y. Liu, "Microstructure evolution, wear behavior, and corrosion performance of alloy steel gradient material fabricated by direct laser deposition," Journal of Materials Research and Technology, vol. 9, no. 5. Elsevier BV, pp. 11702–11716, Sep. 2020. https://doi.org/10.1016/j.jmrt.2020.08.074
25. H. F. Zhang et al., "An investigation on wear and cavitation erosion-corrosion characteristics of the TiC modified Fe-based composite coating via laser cladding," Journal of Materials Research and Technology, vol. 26. Elsevier BV, pp. 8440–8455, Sep 2023. https://doi.org/10.1016/j.jmrt.2023.09.177
26. G. Lu et al., "Tribological performance of functionally gradient structure of graphene nanoplatelets reinforced Ni3Al metal matrix composites prepared by laser melting deposition," Wear, vol. 428–429. Elsevier BV, pp. 417–429, Jun. 2019. https://doi.org/10.1016/j.wear.2019.04.009Y
27. V. Boggarapu, P. S. Rama Sreekanth, and V. B. Peddakondigalla, "Microstructure, mechanical and tribological properties of Al/Cu functionally graded material fabricated through powder metallurgy," Journal of Engineering Research. Elsevier BV, p. 100119, Jun. 2023. https://doi.org/10.1016/j.jer.2023.100119
28. I. Najjar, A. Sadoun, M. N. Alam, and A. Fathy, "Prediction of wear rates of Al-TiO2 nanocomposites using artificial neural network modified with particle swarm optimization algorithm," Materials Today Communications, vol. 35. Elsevier BV, p. 105743, Jun. 2023. https://doi.org/10.1016/j.mtcomm.2023.105743
29. F. Aydin, "The investigation of the effect of particle size on wear performance of AA7075/Al2O3 composites using statistical analysis and different machine learning methods," Advanced Powder Technology, vol. 32, no. 2. Elsevier BV, pp. 445–463, Feb. 2021. https://doi.org/10.1016/j.apt.2020.12.024
30. F. Lin et al., "Characterisation of microstructure, microhardness and tribological properties of Al matrix hybrid nanocomposites reinforced with B4C and in-situ GNSs," Wear, vol. 522. Elsevier BV, p. 204691, Jun. 2023. https://doi.org/10.1016/j.wear.2023.204691
31. E. K. Njim, "Analytical and numerical flexural properties of polymeric porous functionally graded (PFGM) sandwich beams," Journal of Achievements in Materials and Manufacturing Engineering, vol. 110, no. 1. Index Copernicus, pp. 5–10, Jan. 01, 2022.
32. A. Mouthanna, S. H. Bakhy, M. Al-Waily, and E. K. Njim, "Free Vibration Investigation of Single-Phase Porous FG Sandwich Cylindrical Shells: Analytical, Numerical and Experimental Study," Iranian Journal of Science and Technology, Transactions of Mechanical Engineering. Springer Science and Business Media LLC, Aug. 29, 2023.
33. Mahdi. M. S. Sharif, Ahmad. N. Al-Khazraji, Samir. A. Amin, "Flexural Properties of Functionally Graded Polymer Alumina Nanoparticles," Engineering and Technology Journal, Vol. 39, Part A, No. 05, pp. 821-835, 2021.
34. ASTM G65. Standard Test Method for Measuring Abrasion Using the Dry Sand/Rubber Wheel Apparatus.
35. B. K. Yildiz and Y. K. Tur, "Analysis of reciprocating wear behavior of Al2O3 ceramic composites prepared with nano-Ni, ZrO2, and Cr2O3 additives through heterogeneous precipitation," Jurnal Tribologi, vol. 37, pp.29-41. 2023.
36. Bharat Bhushan, "PRINCIPLES AND APPLICATIONS OF TRIBOLOGY," A John Wiley & Sons, Ltd., Publication, 2013.